Acta Crystallographica Section F
Structural Biology and Crystallization Communications
ISSN 1744-3091

Structure of armadillo ACBP: a new member of the acyl-CoA-binding protein family

Marcelo D. Costabel,[a]* Mario R. Ermácora,[b] José A. Santomé,[c] Pedro M. Alzari[d] and Diego M. A. Guérin[e]

[a]Grupo de Biofísica, Departamento de Física, Universidad Nacional del Sur, Bahía Blanca, Argentina, [b]Departamento de Ciencia y Tecnología, Universidad Nacional de Quilmes, Bernal, Argentina, [c]Instituto de Química y Fisicoquímica Biológicas (IQUIFYB), Facultad de Farmacia y Bioquímica (UBA-CONICET), Buenos Aires, Argentina, [d]Unité de Biochimie Structurale, Institut Pasteur, Paris, France, and [e]Unidad de Biofisica (CSIC-UPV/EHU), PO Box 644, E-48080 Bilbao, Spain

Correspondence e-mail: costabel@criba.edu.ar

Received 11 July 2006
Accepted 18 September 2006

PDB Reference: armadillo ACBP, 2fdq, r2fdqsf.

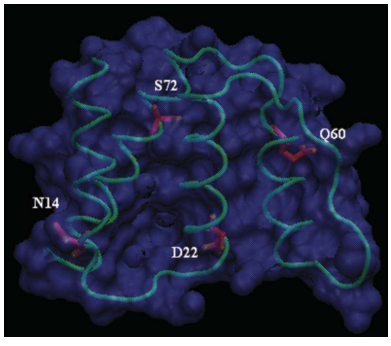

The X-ray structure of the tetragonal form of apo acyl-CoA-binding protein (ACBP) from the Harderian gland of the South American armadillo *Chaetophractus villosus* has been solved. ACBP is a carrier for activated long-chain fatty acids and has been associated with many aspects of lipid metabolism. Its secondary structure is highly similar to that of the corresponding form of bovine ACBP and exhibits the unique flattened α-helical bundle (up–down–down–up) motif reported for animal, yeast and insect ACBPs. Conformational differences are located in loops and turns, although these structural differences do not suffice to account for features that could be related to the unusual biochemistry and lipid metabolism of the Harderian gland.

1. Introduction

Acyl-CoA-binding protein (ACBP) binds CoA thioesters of C_{14}–C_{22} fatty acids (LCFA-CoAs) with nanomolar affinity (Kragelund *et al.*, 1999) and is involved in the intracellular transport and storage of these compounds. Because LCFA-CoAs modulate the activity of several proteins and genes, ACBP also plays an important role in metabolism, cell signalling, membrane biogenesis and gene expression (Faergeman & Knudsen, 1997; Faergeman *et al.*, 2004; Fulceri *et al.*, 1999; Gaigg *et al.*, 2001; Helledie *et al.*, 2002; Knudsen *et al.*, 2000; Kragelund *et al.*, 1999).

Sequence analysis demonstrates that the 10 kDa ACBP domain belongs to a highly conserved family of eukaryotic proteins (Burton *et al.*, 2005) and can be found alone or as part of larger modular proteins (Leung *et al.*, 2006; Suk *et al.*, 1999). NMR and X-ray structures of the stand-alone ACBPs from *Taurus bovis*, *Plasmodium falciparum* and *Saccharomyces cerevisiae* are available (Kragelund *et al.*, 1993; Teilum *et al.*, 2005; van Aalten *et al.*, 2001; PDB codes 1aca, 1st7, 1hb6, 1hb8 and 1hbk). In addition, structures of multidomain proteins containing ACBP modules have been solved (PDB codes 2cqu and 2cop). ACBP adopts a unique open helix-bundle fold (up–down–down–up) with a shallow and exposed cavity that serves as a binding site (Kragelund *et al.*, 1993; Teilum *et al.*, 2005; van Aalten *et al.*, 2001). The fatty-acid part of the ligand lines the cavity and is covered by the solvated adenosine-3′-phosphate moiety.

Comparison of bovine, insect and yeast ACBPs shows a nearly identical architecture of helical elements with conformational variation in the connecting loops. This variation might be related to binding specificity, affinity for different ligands (van Aalten *et al.*, 2001) and crystallographic contacts (see below), as well as to differential interaction with membranes and macromolecules (Vallejo, 2006). The loop between helix 1 and 2, at the rim of the binding site, is of particular interest because it exhibits significant changes in length and sequence among animal, yeast and insect ACBPs and may be related to species differences in ligand selectivity (van Aalten *et al.*, 2001).

Mammalian Harderian glands are lipogenic organs that produce an abundant secretion of glycerol ether lipids. These unique compounds are synthesized by peroxisomal enzymes from a separated pool of LCFA-CoAs (Horie & Suga, 1989). In the Harderian glands of the South American armadillo *Chaetophractus villosus*, the expression

pattern of ACBP is unusual (Cavagnari *et al.*, 2001). This, along with the peculiarities in lipid composition and metabolism, prompted us to characterize the protein (Cavagnari *et al.*, 1997, 2001, 2002). In this study, we report the X-ray structure of armadillo ACBP. Since only a few ACBP structures have so far been reported, the new data should be useful in comparative studies aimed at understanding the function and evolution of these proteins.

2. Materials and methods

Armadillo ACBP was prepared as previously described (Cavagnari *et al.*, 2002); the procedure yields ligand-free highly soluble monomeric protein with >98% purity. The purified protein in 20 m*M* Tris–HCl pH 8.0 was concentrated to 40 mg ml^{-1} using a Centricon YM-3 (Milipore Corp., Bedford, MA, USA). Crystallization trials were carried out using both sitting-drop and hanging-drop vapour-diffusion methods. Crystals were obtained at 277 K using a 1.0 ml reservoir composed of 24%(*w*/*v*) polyethylene glycol 6000, 5% NaCl and 10 m*M* Tris–HCl buffer pH 8.0. Drops contained 60% reservoir solution and 40% 10 mg ml^{-1} protein solution. A single crystal was mounted in a thin-walled quartz capillary and used for data collection. Cu $K\alpha$ X-rays were generated by a Rigaku RU-300 rotating-anode generator operating at 40 kV and 80 mA. Diffraction data were collected at room temperature using a MAR Research image-plate scanner. 100 sequential images were recorded with an oscillation angle of 1.0° per image; data reduction was carried out with *DENZO* and *SCALEPACK* (Otwinowski & Minor, 1997). Molecular replacement, model bulding and refinement were performed with *AMoRe* (Navaza, 2001), *O* (Jones *et al.*, 1991) and *REFMAC*5 (Collaborative Computational Project, Number 4, 1994), respectively. The structure was solved using the program *ARP* (Perrakis *et al.*, 1999) and water molecules not clearly defined were removed manually with *O* (Jones *et al.*, 1991). The quality of intermediate and final models was monitored using *PROCHECK* (Laskowski *et al.*, 1993).

3. Results and discussion

Using the conditions described in §2, long needle-like crystals appeared after 2–3 d. On longer incubation (6–10 d), bipyramidal crystals were observed (0.3 × 0.3 × 0.3 mm; Fig. 1). The bipyramidal crystals exhibited diffraction consistent with the tetragonal space group $P4_1$, with unit-cell parameters $a = b = 49.11$, $c = 130.48$ Å and three molecules in the asymmetric unit. A diffraction data set was collected to 3.5 Å, with a completeness of 100% and an $R_{\rm merge}$ of 13.6%. Data-collection statistics are summarized in Table 1.

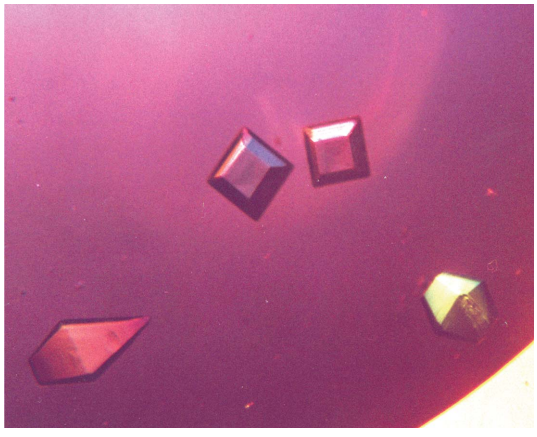

Figure 1
Crystals of armadillo ACBP. The crystals are approximately 0.3 × 0.3 × 0.3 mm in size.

Table 1
Data collection and refinement.

Values in parentheses refer to the outermost shell (3.62–3.50 Å).

Space group	$P4_1$
Unit-cell parameters (Å, °)	$a = b = 49.11$, $c = 130.48$, $\alpha = \beta = \gamma = 90.0$
Resolution range (Å)	25.0–3.50
Unique reflections	3901
Completeness (%)	100 (99.5)
$\langle I/\sigma(I)\rangle$	12.9 (5.29)
$R_{\rm merge}$ (%)	13.6 (26.2)
No. of molecules in ASU	3
No. of protein atoms	2125
No. of solvent molecules	37
$R_{\rm cryst}$† (%)	19.5
$R_{\rm free}$ (10% of data) (%)	25.7
R.m.s. deviations from ideality	
Bond lengths (Å)	0.008
Angles (°)	1.5
Ramachandran statistics	
Residues in most favoured regions	180 [77.9%]
Residues in additional allowed regions	48 [20.8%]
Residues in generously allowed regions	1 [0.4%]
Residues in disallowed regions	2 [0.9%]

† $R = \sum_{hkl}[|F_{\rm o}(hkl) - kF_{\rm c}(hkl)|/\sum_{hkl} F_{\rm o}(hkl)]$.

The search model was the crystal structure of bovine ACBP (PDB code 1hb8). A solution was found with space group $P4_1$ or $P4_3$ and a CC of 0.621 (R factor 0.510) within the resolution range 15–30 Å. Examination of the crystal packing revealed that space group $P4_3$ produced superpositions between symmetry-related molecules whereas the enantiomorph $P4_1$ did not, implying that the correct solution corresponded to $P4_1$. By alternating simulated annealing, manual rebuilding and addition of solvent molecules, the model was further refined. The final model has an R factor of 0.195 ($R_{\rm free}$ = 0.257), displays good stereochemistry with only one residue (Met46) in a disallowed region of the Ramachandran statistics and contains 37 water molecules.

Although some disorder can be seen in a few solvent-exposed side chains, the backbone and most side chains are well defined in the electron-density map. The solved structure (PDB code 2fdq) is a bundle of four helices (residues 2–12, 21–35, 49–60 and 66–84) with an up–down–down–up topology (Fig. 2). The overall structure is nearly identical to that of bovine ACBP (PDB code 1hb8): the pairwise r.m.s.d. after superposition on CA atoms is less than 0.4 Å, with most of the variation concentrated in the connecting turns and loops.

This newest structure reveals local conformational changes to accommodate the four residue differences between bovine and armadillo ACBP variants (Fig. 2). Of particular interest is the substitution of His for Asn at position 14 in the loop connecting helix 1 and 2, which perturbs the backbone and may have an impact on the fine-tuning of ligand selectivity. The r.m.s.d. between the two structures at position 14 is 0.7 Å, distinctly larger than the mean for the complete structure. Another interesting feature observed in the present structure is the conformational variability of the loop containing Met46 as well as that of the residue itself. In the structure of the orthorhombic crystal form of bovine ACBP this region is a type I turn, whereas it is a type II turn (Venkatachalam, 1968) in the tetragonal form. This causes the side chain of Met46 to point in opposite directions, suggesting that the Met46 side chain can adopt many possible orientations. The difference between the two crystal

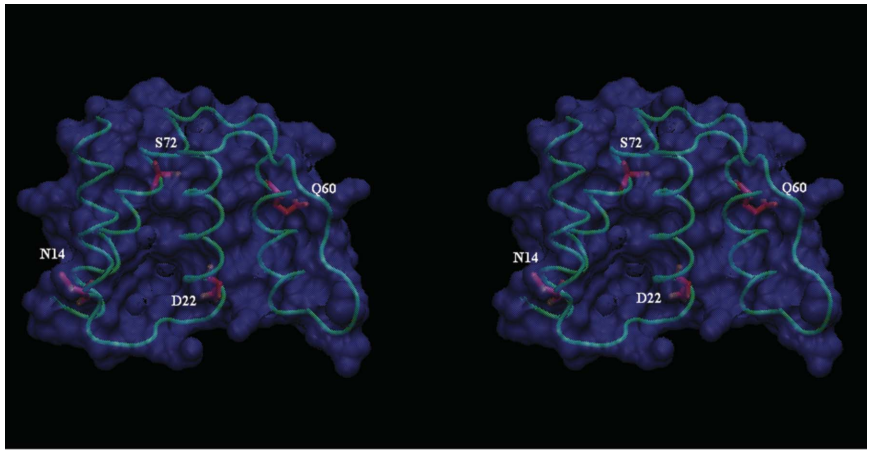

Figure 2
Stereo image of the crystal structure of armadillo ACBP. Amino acids shown as stick models correspond to sequence differences between armadillo and bovine ACBP. The largest conformational difference between these two proteins is in the loop containing Asn14 (see text).

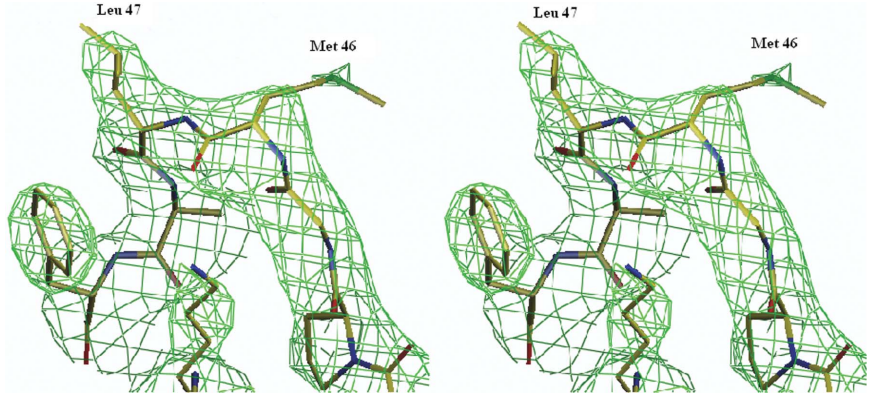

Figure 3
Stereo image of the loop containing the surface-exposed residues Met46 and Leu47.

forms was ascribed to steric restrictions imposed by the contacts between the three molecules in the asymmetric unit. In the armadillo ACBP the 45–48 section of the backbone adopts a type II β-turn (Fig. 3), which is consistent with the crystal-packing hypothesis. Nevertheless, this conformational flexibility uncovers the ability of this protein to oscillate between two conformations that may be of functional interest. In fact, it was observed by simulation that this turn (and particularly Met46) is involved in ACBP ligand binding (Vallejo, 2006). It is worth noting that in the tetragonal form of both bovine (van Aalten *et al.*, 2001) and armadillo ACBP the Met46 dihedral angles are in a disallowed region of the Ramachandran plot. Similarly, in the NMR structure of apo bovine ACBP Asp48 is in a disallowed region of the plot, building a conformational tension that is absent in ligand-bound ACBP (Kragelund *et al.*, 1993). Taken together, these results may indicate that the turn 45–48 is involved in the conformational events associated with ligand transactions between lipid bilayers and ACBP.

Overall, the structure of the ACBP from armadillo Harderian gland has been solved and shows the same fold as the other known ACBP structures (van Aalten *et al.*, 2001; Teilum *et al.*, 2005; Kragelund *et al.*, 1993). One difference is in the loop that contains residue 14, where a change of His for Asn affects the conformation in a protein region that may be related to ligand selectivity (van Aalten *et al.*, 2001). Another feature confirmed by the armadillo ACBP structure is the conformational variability of Met46, although the relationship between the above structural features and the peculiar lipid biochemistry in Harderian glands remains to be established. The data reported herein should be valuable in the systematic analysis of the structure–function relationship and conformational variation within the ACBP family of proteins as a whole.

We thank D. Vallejo and J. R. Grigera for helpful discussions and D. Milikowski and B. Cavagnari for technical assistance. MRE is a member of the National Research Council of Argentina (CONICET). This work was partially supported by a SECYT-UNS 24/F035 grant.

References

van Aalten, D. M., Milne, K. G., Zou, J.-Y., Kleywegt, G. J., Bergfors, T., Ferguson, M. A., Knudsen, J. & Jones, T. A. (2001). *J. Mol Biol.* **309**, 181–192.
Burton, M., Rose, T. M., Faergeman, N. J. & Knudsen, J. (2005). *Biochem. J.* **392**, 299–307.
Cavagnari, B. M., Cordoba, O. L., Affanni, J. M. & Santome, J. A. (1997). *Comput. Biochem. Physiol. B Biochem. Mol. Biol.* **118**, 173–180.
Cavagnari, B. M., Milikowski, D., Haller, J. F., Zanek, M. C., Santome, J. A. & Ermacora, M. R. (2002). *Int. J. Biol. Macromol.* **31**, 19–27.
Cavagnari, B. M., Sterin-Speziale, N., Affanni, J. M., Knudsen, J. & Santome, J. A. (2001). *Biochim. Biophys. Acta*, **1545**, 314–325.
Collaborative Computational Project, Number 4 (1994). *Acta Cryst.* D**50**, 760–763.

Faergeman, N. J., Feddersen, S., Christiansen, J. K., Larsen, M. K., Schneiter, R., Ungermann, C., Mutenda, K., Roepstorff, P. & Knudsen, J. (2004). *Biochem. J.* **380**, 907–918.
Faergeman, N. J. & Knudsen, J. (1997). *Biochem. J.* **323**, 1–12.
Fulceri, R., Giunti, R., Knudsen, J., Leuzzi, R., Kardon, T. & Benedetti, A. (1999). *Biochem. Biophys. Res. Commun.* **264**, 409–412.
Gaigg, B., Neergaard, T. B., Schneiter, R., Hansen, J. K., Faergeman, N. J., Jensen, N. A., Andersen, J. R., Friis, J., Sandhoff, R., Schroder, H. D. & Knudsen, J. (2001). *Mol. Biol. Cell*, **12**, 1147–1160.
Helledie, T., Jorgensen, C., Antonius, M., Krogsdam, A. M., Kratchmarova, I., Kristiansen, K. & Mandrup, S. (2002). *Mol. Cell. Biochem.* **239**, 157–164.
Horie, S. & Suga, T. (1989). *Biochem. J.* **262**, 677–680.
Jones, T. A., Zou, J.-Y., Cowan, S. W. & Kjeldgaard, M. (1991). *Acta Cryst.* A**47**, 110–119.
Knudsen, J., Neergaard, T. B., Gaigg, B., Jensen, M. V. & Hansen, J. K. (2000). *J. Nutr.* **130**, 294S–298S.
Kragelund, B. B., Andersen, K. V., Madsen, J. C., Knudsen, J. & Poulsen, F. M. (1993). *J. Mol. Biol.* **230**, 1260–1277.
Kragelund, B. B., Knudsen, J. & Poulsen, F. M. (1999). *Biochim. Biophys. Acta*, **1441**, 150–161.
Laskowski, R. A., MacArthur, M. W., Moss, D. S. & Thornton, J. M. (1993). *J. Appl. Cryst.* **26**, 283–291.
Leung, K. C., Li, H. Y., Xiao, S., Tse, M. H. & Chye, M. L. (2006). *Planta*, **223**, 871–881.
Navaza, J. (2001). *Acta Cryst.* D**57**, 1367–1372.
Otwinowski, Z. & Minor, W. (1997). *Methods Enzymol.* **276**, 307–326.
Perrakis, A., Morris, R. & Lamzin, V. S. (1999). *Nature Struct. Biol.* **6**, 458–463.
Suk, K., Kim, Y. H., Hwang, D. Y., Ihm, S. H., Yoo, H. J. & Lee, M. S. (1999). *Biochim. Biophys. Acta*, **1454**, 126–131.
Teilum, K., Thormann, T., Caterer, N. R., Poulsen, H. I., Jensen, P. H., Knudsen, J., Kragelund, B. B. & Poulsen, F. M. (2005). *Proteins*, **59**, 80–90.
Vallejo, D. (2006). Personal communication.
Venkatachalam, C. M. (1968). *Biopolymers*, **6**, 1425–1436.